Bone marrow transplantation alters lung antigen-presenting cells to promote T_H17 response and the development of pneumonitis and fibrosis following gammaherpesvirus infection

X Zhou[1], H Loomis-King[1], SJ Gurczynski[1], CA Wilke[1], KE Konopka[2], C Ptaschinski[2], SM Coomes[3], Y Iwakura[4], LF van Dyk[5], NW Lukacs[2] and BB Moore[1,6]

Hematopoietic stem cell transplantation (HSCT) efficacy is limited by numerous pulmonary complications. We developed a model of syngeneic bone marrow transplantion (BMT) followed by infection with murine gamma herpesvirus-68 that results in pneumonitis and fibrosis and mimics human "noninfectious" HSCT complications. BMT mice experience increased early lytic replication, but establish viral latency by 21 days post infection. CD4 T cells in BMT mice are skewed toward interleukin (IL)-17A rather than interferon (IFN)-γ production. Transplantation of bone marrow from *Il-17a*$^{-/-}$ donors or treatment with anti-IL-17A neutralization antibodies at late stages attenuates pneumonitis and fibrosis in infected BMT mice, suggesting that hematopoietic-derived IL-17A is essential for development of pathology. IL-17A directly influences activation and extracellular matrix production by lung mesenchymal cells. Lung CD11c + cells of BMT mice secrete more transforming growth factor beta-β1, and pro-T_H17 mRNAs for IL-23 and IL-6, and less T_H1-promoting cytokine mRNA for IFN-γ but slightly more IL-12 mRNA in response to viral infection. Adoptive transfer of non-BMT lung CD11c-enriched cells restores robust T_H1 response and suppresses aberrant T_H17 response in BMT mice to improve lung pathology. Our data suggest that "noninfectious" HSCT lung complications may reflect preceding viral infections and demonstrate that IL-17A neutralization may offer therapeutic advantage even after disease onset.

INTRODUCTION

Hematopoietic stem cell transplantation (HSCT) is a potentially curative therapy for inherited genetic disorders, autoimmune diseases, and malignancies. However, the usefulness of this therapy is limited by the development of lung complications, which occur in 30–60% of HSCT patients, and are associated with significant morbidity and mortality.[1,2] During HSCT, a recipient may receive hematopoietic stem cells from a histocompatibility antigen-matched donor or from him/herself (allogeneic or autologous HSCT). Recent multi-country surveys found that ~42% of the HSCT procedures are allogeneic, whereas ~58% are autologous HSCT.[3]

Pulmonary complications (infectious and noninfectious) can occur in both allogeneic and autologous HSCT, but tend to be more frequent in allogeneic HSCT recipients.[1] Infectious pneumonia can be caused by fungi, bacteria, or viruses and can occur even after full hematopoietic reconstitution.[4] The occurrence of noninfectious pulmonary complications follows a characteristic time pattern.[1,2] Engraftment syndrome, diffuse alveolar hemorrhage, and periengraftment respiratory distress syndrome usually occur during the first 30 days following transplant. Bronchiolitis obliterans syndrome (BOS) and cryptogenic organizing pneumonia (COP) usually occur late post-transplantation.[5] Nonspecific interstitial fibrosis can also occur during the late post-transplant period.[2,6] Idiopathic

[1]Department of Internal Medicine, Pulmonary and Critical Care Medicine Division, University of Michigan, Ann Arbor, Michigan, USA. [2]Department of Pathology, University of Michigan, Ann Arbor, Michigan, USA. [3]Graduate Program in Immunology, University of Michigan, Ann Arbor, Michigan, USA. [4]Research Institute for Biomedical Sciences, Tokyo University of Science, Noda, Chiba, Japan. [5]Department of Immunology and Microbiology, University of Colorado School of Medicine, Aurora, Colorado, USA and [6]Department of Microbiology and Immunology, University of Michigan, Ann Arbor, Michigan, USA. Correspondence: B Moore (Bmoore@umich.edu)

Received 15 April 2015; accepted 31 July 2015; published online 16 September 2015. doi:10.1038/mi.2015.85

pneumonia syndrome (IPS) can occur at any time following transplant.[7] Late-stage complications that manifest following hematopoietic reconstitution result in severe and often fatal lung dysfunction.[2] Unfortunately, the etiology and pathogenesis of IPS, BOS, COP, and nonspecific interstitial fibrosis are all poorly understood.

Noninfectious late complications are often diagnosed by the absence of apparent infection at the time of symptom onset, although recent evidence suggests some cases of IPS may have occult infections.[8] In addition, these complications may represent pathologic sequelae that are initially triggered by a preceding viral infection even if the lytic infection is cleared by the time of diagnosis.[9,10] For example, a prospective study of pediatric allogeneic HSCT recipients found that early respiratory virus infection post-HSCT was correlated significantly with the later development of IPS and BOS.[10] Many of the noninfectious complications including IPS, BOS, and COP manifest with lung fibrosis, a scarring process that excessively deposits extracellular matrix, especially collagen, causing stiffness and reducing oxygen diffusion capacity at the later stages.[2] In general, lung fibrosis is believed to represent a dysregulated wound-healing response to lung injury. Viral infections have been suggested to mediate lung injury that leads to some forms of pulmonary fibrosis.[11] For example, Epstein–Barr virus, cytomegalovirus (CMV), human herpes viruses-7, and Kaposi's sarcoma-associated herpesvirus are often found in lung tissue of human familial and idiopathic pulmonary fibrosis patients (reviewed in ref. 11). In addition, infection with murine gamma herpesvirus-68 (γHV-68) can lead to fibrosis in aged or Th2-biased mice.[11] To determine whether gammaherpesvirus can contribute to the development of lung dysfunction in the context of HSCT, we previously established a murine model of infection following bone marrow transplantation (BMT). In this model, fully hematopoietic reconstituted syngeneic or allogeneic BMT mice are infected with murine γHV-68, which is genetically related to human Epstein–Barr virus and Kaposi's sarcoma-associated herpesvirus.[12,13] Allogeneic BMT mice die starting by day 10 when infected with γHV-68; however, syngeneic BMT (hereafter referred to as just BMT) mice infected with γHV-68 develop interstitial pneumonitis and fibrosis that persists after lytic viral infection has been cleared, at a time point when the virus has established latency[12] (**Supplementary Figure 1** online). The inflammatory and fibrotic pathology that develops in these mice shares features of IPS, BOS, COP, and nonspecific fibrosis that also complicate human HSCT.

In our γHV-68-infected BMT mouse pneumonitis and fibrosis model, we previously demonstrated an increase in the percentage of CD4 T cells that produce interleukin (IL)-17A and a concomitant reduction in CD4 cells producing interferon (IFN)-γ.[12] In this study, we aimed to investigate the mechanisms that underlie the development of pneumonitis and fibrosis in fully reconstituted BMT mice after γHV-68 infection. Here we report that transplantation of bone marrow cells from *Il-17a*$^{-/-}$ mice or neutralization of IL-17A greatly attenuated pneumonitis and fibrosis induced by γHV-68 infection in BMT mice. Lung antigen-presenting cells (APCs) are critical in priming T helper cells to differentiate into T_H17 cells by producing increased amounts of transforming growth factor-β1, IL-6, and IL-23 post HSCT in response to γHV-68. IL-17A has direct effects on fibroblasts by stimulating their proliferation and extracellular matrix secretion. Thus, this model allows us to understand how innate and adaptive immune responses to a respiratory virus are altered in the setting of HSCT and provide insight into potential etiologies of "noninfectious" pulmonary complications following HSCT therapy.

RESULTS

BMT mice are impaired in restricting γHV-68 lytic replication and develop pulmonary fibrosis by 21 dpi

To understand viral host defense and pulmonary complications post HSCT, we have developed a BMT mouse model.[12,13] Recipient C57BL/6 mice are lethally irradiated followed by syngeneic BMT. Hematopoietic reconstitution of the periphery and lung is complete by 5 weeks post BMT when assessed by CD45.1 and CD45.2 haplotypes;[14] thus, viral infection with γHV-68 occurs at a time of full hematopoietic reconstitution. We infected mice with recombinant γHV-68 harboring an EYFP-tagged histone H2B to allow quantitation of the numbers of infected cells.[15] In BMT mice, viral-infected cells were detectable starting at 3 days post infection (dpi), with most infected cells appearing in clusters, especially near airways, indicating active replication and transmission of virus (**Figure 1a**). In non-BMT mice, infected cells were rarely detectable until 7 dpi, with scattered infected cells indicating limited cell to cell infection (**Figure 1a**). There were significantly more viral-infected cells in BMT lungs than in non-BMT lungs at both 3 and 7 dpi (**Figure 1b**). At 21 dpi, both BMT and non-BMT mice had few EYFP-H2b-positive cells; confirming that both BMT and non-BMT mice had established a latent infection by 21 dpi.[12]

To quantify differences in early viral lytic replication between BMT and non-BMT mice, mRNA was isolated from both groups of mice at designated dpi, and real-time reverse transcriptase PCR was performed to measure lytic viral gene expression. An ~140-fold increase in the expression of viral DNA polymerase (**Figure 1c**) and envelope glycoprotein gene *gB* (data not shown) was detected at 3 dpi in BMT mice but this difference was reduced to about threefold at 7 dpi (**Figure 1c**), consistent with our earlier report.[13] BMT mice experience increased lung injury post infection in response to the viral replication within the first 7 dpi as noted by an increase in the protein concentration in the bronchoalveolar lavage fluid (**Supplementary Figure 2a**). The virus establishes latency by 14 dpi[16] and maintains latency through 21 dpi in both BMT and non-BMT mice,[12,16] with little lytic gene expression detectable at this time point (**Figure 1c**).

Reactivation of γHV-68 is not required to develop pulmonary fibrosis in BMT mice

Pulmonary fibrosis can be induced by γHV-68 in T_H2-biased *IFN-γR*$^{-/-}$ mice through reactivation of latent virus.[17] To determine whether reactivation of latent γHV-68 in BMT lungs is important for the development of pulmonary fibrosis, we

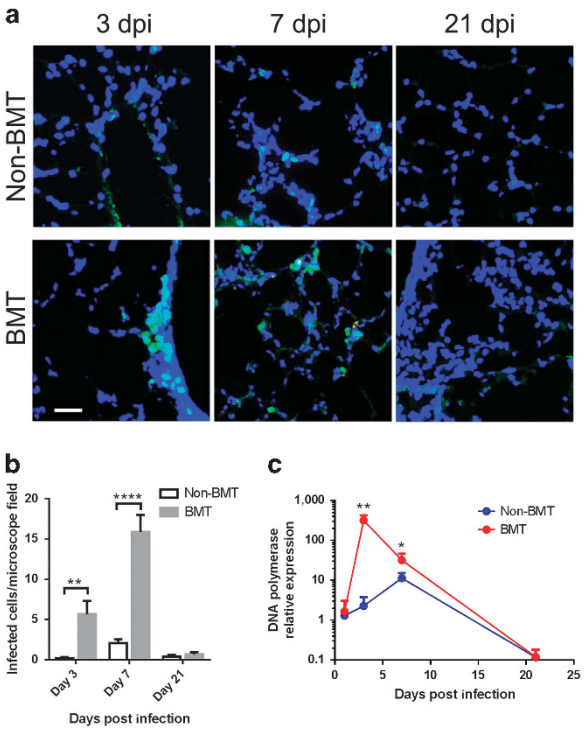

Figure 1 BMT mice cannot efficiently restrict gammaherpesvirus lytic replication. (**a**) Representative lung sections from $n=3$ syngeneic BMT C57BL/6J mice or age-matched non-BMT mice infected with 5×10^4 pfu γHV-68-H2bYFP intranasally and analyzed by histology at 3, 7, or 21 dpi (bars = 40 μm, same magnification for the images). H2bYFP expressed in viral-infected cells was detected by a cross-reactive fluorescein isothiocyanate (FITC)-conjugated anti-GFP antibody (green). DAPI nuclear counterstains are blue. (**b**) YFP-positive virus-infected cell count per microscope field under × 1000 magnification (mean + s.e.m., $n=10$). A typical field has ~ 250 cells in total. Data are pooled from two independent experiments. $^{**}P<0.01$ and $^{****}P<0.0001$. (**c**) γHV-68 lytic replication in BMT or non-BMT mice at designated time points post infection as measured by relative mRNA abundance of viral DNA polymerase (mean + s.e.m., $n=5$). $^{*}P<0.05$ and $^{**}P<0.01$, $^{****}P<0.0001$. Similar results were obtained in two additional experiments.

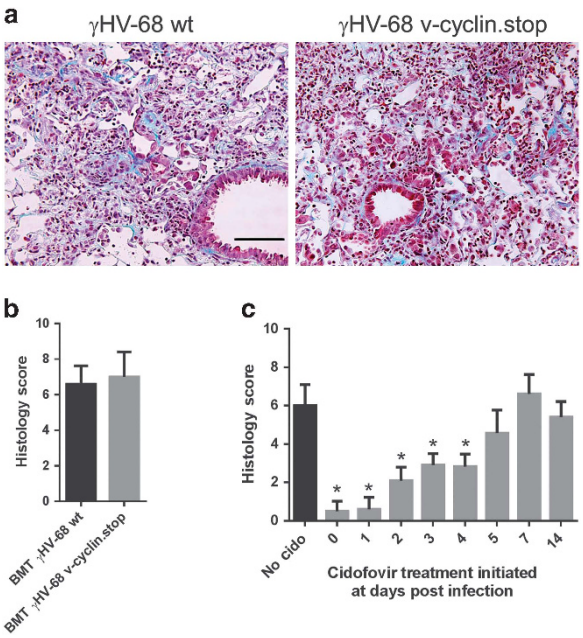

Figure 2 Viral reactivation is not required for the development of pneumonitis and lung fibrosis in BMT mice. (**a**) Representative lung sections from BMT mice infected with either a γHV-68 mutant containing a stop codon within ORF 72 (v-cyclin.stop) or the WT virus at 21 dpi. The lung sections were stained with Masson's trichrome, and blue staining represents deposition of collagen. Same magnification for both images (bar = 100 μm), (**b**) The average histology scores of lung sections from v-cyclin.stop or wild-type virus-infected BMT mice at 21 dpi (mean + s.e.m., $n=5$). Lung sections were scored on an 11 point scale as in Methods. (**c**) Average histology scores of lung sections from γHV-68-infected BMT mice with or without cidofovir treatment starting at designated days post viral infection (mean + s.e.m., $n=5$). Cidofovir was administered subcutaneously at a dose of 25 mg kg^{-1} of body weight. Mice were treated with cidofovir for 2 consecutive days and then were injected in every 3 days until 21 dpi. $^{*}P<0.05$. Similar results were obtained in two additional experiments.

infected BMT mice with either a γHV-68 mutant containing a stop codon within ORF 72 (v-cyclin.stop)[18] or the wild-type (WT) virus. The v-cyclin.stop virus undergoes normal lytic replication during acute infection but has greater than a 100-fold reduction in the ability to reactivate from latency.[18] At 21 dpi, v-cyclin.stop viruses caused pulmonary fibrosis that was just as severe as the WT virus (**Figure 2a,b**). Thus, γHV-68 viral reactivation is not required for the development of pulmonary fibrosis in BMT mice. To further define the window during which viral lytic replication is critical for later fibrotic pathology, we treated γHV-68-infected BMT mice with cidofovir, a nucleoside analog that competitively inhibits the incorporation of deoxycytidine triphosphate into viral DNA by viral DNA polymerase,[19] starting at various time points. Administration of cidofovir before 4 dpi significantly protected BMT mice from development of pneumonitis and pulmonary fibrosis at 21 dpi, whereas administration of cidofovir after 4 dpi had no significant effect as noted in the pathologic scoring of tissues (**Figure 2c**).

Infected BMT mice are characterized by increased T_H17 and decreased T_H1 differentiation

We next compared the kinetics of helper T-cell differentiation in infected non-BMT and BMT mice. In BMT mice, the percent of T_H1 cells (expressing IFN-γ) was significantly decreased at 7 and 14 dpi, whereas the percent of T_H17 cells (expressing IL-17A) was continuously increased at 7, 14, and 21 dpi (**Figure 3a,b**). There was no significant difference among non-BMT and BMT mice in T_H2 differentiation as determined by percent of IL-4 expressing cells (**Figure 3c**). Given the accumulation of T_H17 cells over time in this model, we next addressed the impact of IL-17A on the disease pathogenesis.

Bone marrow-derived IL-17A-producing cells are required for the development of pneumonitis and fibrosis in γHV-68-infected BMT mice

To determine whether the increase in T_H17 cells in BMT mice is responsible for the development of lung pathology post infection, we transplanted bone marrow of *Il-17a*$^{-/-}$ mice on a C57BL/6 background[20] into C57BL/6 mice, confirmed full

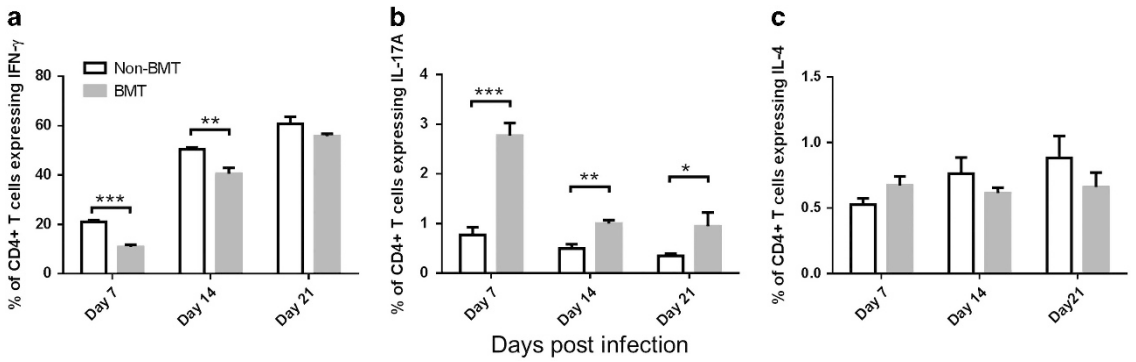

Figure 3 Increased T_H17 cells and decreased T_H1 cells are found in BMT mice post γHV-68 infection. Single cell suspensions were prepared by collagenase digestion of whole lungs of non-BMT control or BMT mice at 7, 14, or 21 dpi with γHV-68. Cells were then stimulated with phorbol 12-myristate 13-acetate (PMA) and ionomycin and analyzed by flow cytometry. $CD45^+$ $CD4^+$ cells were gated. (**a**) Percent of CD4+ cells that express IFN-γ (T_H1 cells); (**b**) percent of CD4+ cells that express IL-17A (T_H17 cells); (**c**) percent of CD4+ cells that express IL-4 (T_H2 cells). $^*P<0.05$, $^{**}P<0.01$, $^{***}P<0.001$. Data are pooled from two independent experiments (Mean + s.e.m., $n=7$).

hematopoietic reconstitution (5 weeks) and then infected with γHV-68. We saw striking protection from pneumonitis and fibrosis in the mice that received *Il-17a*$^{-/-}$ bone marrow at 21 dpi (**Figure 4a,b**). To determine whether a somatic source of IL-17A is necessary for the development of lung pathology, we transplanted marrow of WT mice into *Il-17a*$^{-/-}$ mice and then infected with γHV-68. These mice were not protected from pneumonitis or fibrosis (**Figure 4a,b**). To determine whether IL-17A has any impact on acute viral replication in either BMT or non-BMT mice, we infected WT or *Il-17a*$^{-/-}$ mice or BMT mice (WT into WT vs. *Il-17a*$^{-/-}$ into WT) with γHV-68 and measured acute lytic viral replication. The loss of IL-17A did not impact acute viral replication in either non-BMT or BMT mice (**Figure 4c**).

To determine whether IL-17A was promoting lung pathology via early or late actions, we administrated virally infected BMT mice with neutralizing antibodies against IL-17A[21] either during the priming phase (0–4 dpi) or during the effector phase (after 10 dpi) (**Figure 4d**). Mice receiving neutralizing antibodies against IL-17A during late time points were protected from pulmonary pathology, whereas the ones receiving antibodies during early time points were not (**Figure 4e**).

IL-17A directly activates lung mesenchymal cells

Lung mesenchymal cells, including fibroblasts and fibrocytes, are major contributors to pulmonary fibrotic processes. IL-17A receptor is expressed in mesenchymal cells.[22] To determine whether IL-17A has direct effects on mesenchymal cells, we cultured lung mesenchymal cells isolated from C57Bl/6 mice with recombinant murine IL-17A in various concentrations. IL-17A can significantly increase mesenchymal cell proliferation as measured by uptake of ^{3}H-thymidine (**Figure 5a**). In addition, when murine mesenchymal cells were co-cultured with IL-17A, we observed that the expression of collagen type III and fibronectin first increased at 48 h (**Figure 5b**) followed by increased expression of collagen type I at 72 h (**Figure 5c**).

Lung APCs dictate T_H17 polarization in BMT mice

Pulmonary dendritic cells (DC), rather than alveolar macrophages, are believed to be the major APCs in the lung,[23] although both express CD11c. We thus compared the characteristics of CD11c+ lung APCs from BMT and non-BMT mice. Previously, we found that lung-derived APCs from BMT mice expressed similar levels of MHC class II and co-stimulatory molecules, and were able to effectively stimulate mixed lymphocyte responses,[13] but their cytokine profiles were not characterized. We enriched lung APCs at 7 dpi by collecting $CD11c^+$ cells from collagenase digested lungs; alveolar macrophages were minimized from this population by allowing them to adhere to culture plates. Enriched lung APCs were restimulated with γHV-68 for 36 h to determine their ability to produce pro-T_H17 cytokines. Indeed, APCs from infected BMT mice made significantly more transforming growth factor-β1 and IL-6 and IL-23 mRNA (**Figure 6a**). Although lung APCs from infected BMT mice expressed lower mRNA levels of the pro-T_H1 cytokine IFN-γ, they expressed slightly higher levels of IL-12 mRNA (**Figure 6b**). Lung APCs from unchallenged mice also made more IL-6, IL-23, and IL-1β mRNA than those from non-BMT mice when infected with equivalent doses of virus *ex vivo* for 24 h (**Figure 6c**). Taken together, the differences in cytokine expression levels between the lung APCs from non-BMT and BMT mice are consistent with the skewing of T helper-cell differentiation in BMT mice.

To determine whether T-cell polarization could be directly attributed to lung APC function, we collected CD11c+ lung APCs from either non-BMT or BMT mice at 3 dpi, and adoptively transferred 5×10^5 $CD11c^+$-enriched cells from non-BMT mice into BMT mice, or transferred $CD11c^+$-enriched cells from BMT mice into non-BMT mice (**Figure 7a**). The CD11c+ MHC class II+ APCs in this population were classified by flow cytometry to contain ~65% CD11b+ conventional DCs, 4% CD103+ conventional DCs, 18% Ly6C+ inflammatory DCs, and 16% alveolar macrophages, whereas the $CD11c^{dim}$ plasmacytoid DCs (PDCA1+) were not detected within this population (**Figure 7b**). The CD11c+ cells enriched from BMT lungs had a similar composition of cell types as those cells from non-BMT lungs and the total numbers of CD11c+ APCs that accumulated in BMT and non-BMT mice were similar (data not shown). One day post adoptive

transfer, these mice were infected with γHV-68, and lungs were harvested at 7 dpi for T_H cytokine analysis. Strikingly, BMT mice receiving APCs from non-BMT mice showed increased T_H1 and reduced T_H17 differentiation (**Figure 7c**). However, non-BMT mice receiving APCs from BMT mice maintained normal T helper-cell differentiation. The BMT mice receiving APCs from non-BMT mice were protected from pneumonitis and fibrosis at 21 dpi (**Figure 7d,e**).

DISCUSSION

BMT mice experience increased early lytic viral replication, which is essential for the development of lung pathology, because cidofovir treatment in the first 4 dpi can protect BMT mice from pneumonitis and fibrosis. How early lytic replication promotes eventual lung pathology is not clear. It is possible that increased viral replication causes BMT mice to experience increased lung injury post infection. BMT mice do show evidence of lung injury in response to viral replication within the first 7 dpi as noted by increased protein concentration in the bronchoalveolar lavage fluid, which is minimized if mice are treated simultaneously with cidofovir starting 1 day after infection (**Supplementary Figure 2a**). This is consistent with previous observations that the absolute viral load impacts the degree of pneumonitis and fibrosis in BMT mice;[12] infection with 1×10^3 plaque-forming units γHV-68 results in less lung pathology than 5×10^4 or 1×10^6 plaque-forming units. Interestingly, WT BMT and *Il-17a*$^{-/-}$ into WT BMT mice experience similar levels of viral replication (**Figure 4c**), and similar levels of acute lung injury (**Supplementary Figure 2b**) but the BMT mice with *Il-17a*$^{-/-}$ bone marrow do not develop pneumonitis and fibrosis (**Figure 4a**), indicating lung injury in the absence of IL-17A is insufficient to drive the eventual lung pathology. We believe early viral replication by itself is not sufficient to drive lung pathology, but may be important in recruiting and priming lung APCs to promote the eventual T_H17 responses.

BMT mice develop an altered adaptive immune response to γHV-68. Previous studies have suggested a T_H1-dominant response for γHV-68 clearance in non-transplant mice.[24] We found that T_H1 cells are diminished in the first 14 dpi in BMT mice and T_H17 cells are increased throughout 21 dpi. Our results using IL-17A-deficient mice and anti-IL-17A antibodies suggest bone marrow-derived IL-17A is essential for lung pathology in infected BMT mice. Interestingly, production of IL-17A does not impact replication of γHV-68 in either the non-BMT or the BMT setting. The fact that BMT and non-BMT mice both had few EYFP-H2b-expressing cells evident at

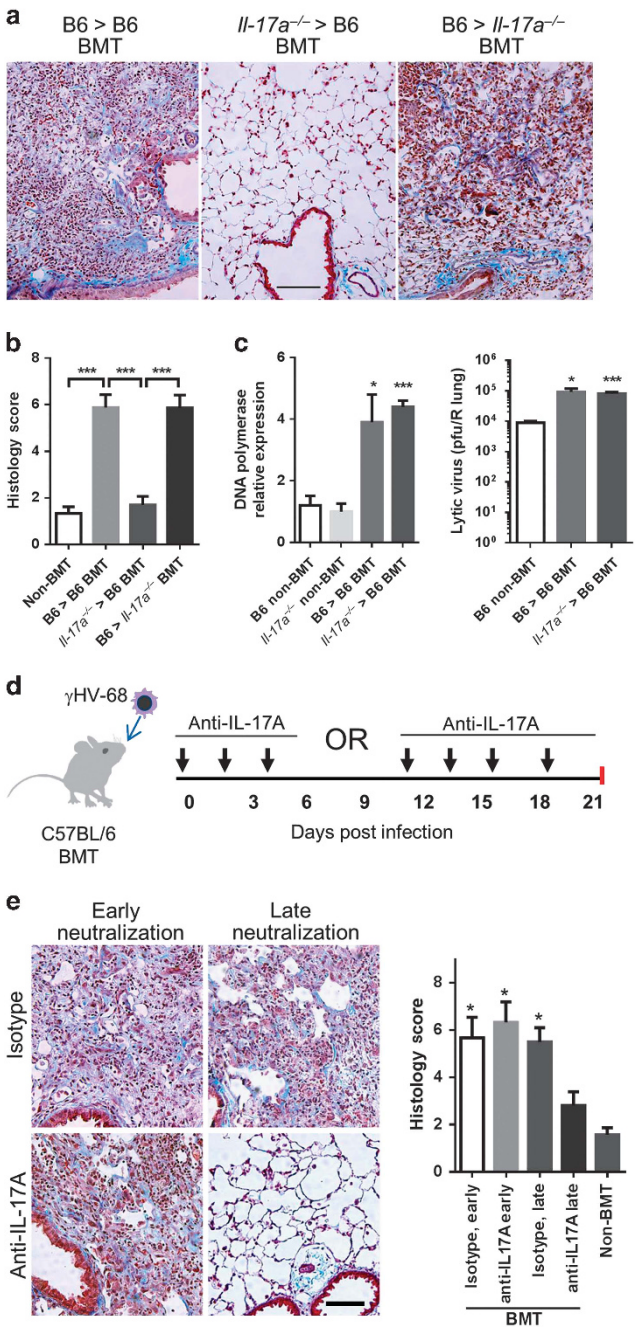

Figure 4 Bone marrow-derived IL-17A is required for the development of pneumonitis and fibrosis in γHV-68-infected BMT mice. (**a**) Representative Masson's trichrome staining of lung sections from WT and *Il-17a*$^{-/-}$ BMT chimeric mice infected with γHV-68 virus at 21 dpi. The blue staining represents deposition of collagen. Same magnification for all images (bar = 100 μm). (**b**) The average histology scores of lung sections from γHV-68-infected non-BMT or BMT mice as described in (**a**) at 21 dpi (mean + s.e.m., $n = 5$). (**c**) Lytic replication of γHV-68 in non-BMT WT or *Il-17a*$^{-/-}$, and in WT recipients of WT grafts or *Il-17a*$^{-/-}$ grafts at 7 dpi. Left, mRNA abundance of viral DNA polymerase as measured by RT-PCR (mean + s.e.m., $n = 5$); right, the number of lytic virus per right lung was directly measured by plaque assay (mean + s.e.m., $n = 5$). Each group was compared with WT non-BMT mice. (**d**) A scheme of γHV-68 infection and subsequent administration of IL-17A neutralization antibodies in WT BMT mice. (**e**) The requirement of IL-17A for development of pneumonitis and fibrosis in BMT mice during late stages. Left, representative Masson's trichrome staining of lung sections from antibody treated BMT mice at 21 dpi. BMT mice received anti-IL-17A antibodies or isotype treatment at early or late time points as shown in (**d**). The blue staining represents deposition of collagen. Right, average histology scores of lung sections from γHV-68 infected non-BMT or BMT mice treated with anti-IL-17A antibodies or isotype (mean + s.e.m., $n = 4$). Each group was compared with BMT mice treated with anti-IL-17A antibodies at late time points. $^*P < 0.05$ and $^{***}P < 0.001$. Similar results were seen in two additional experiments (**a**,**b**) or one additional experiment (**c**,**e**).

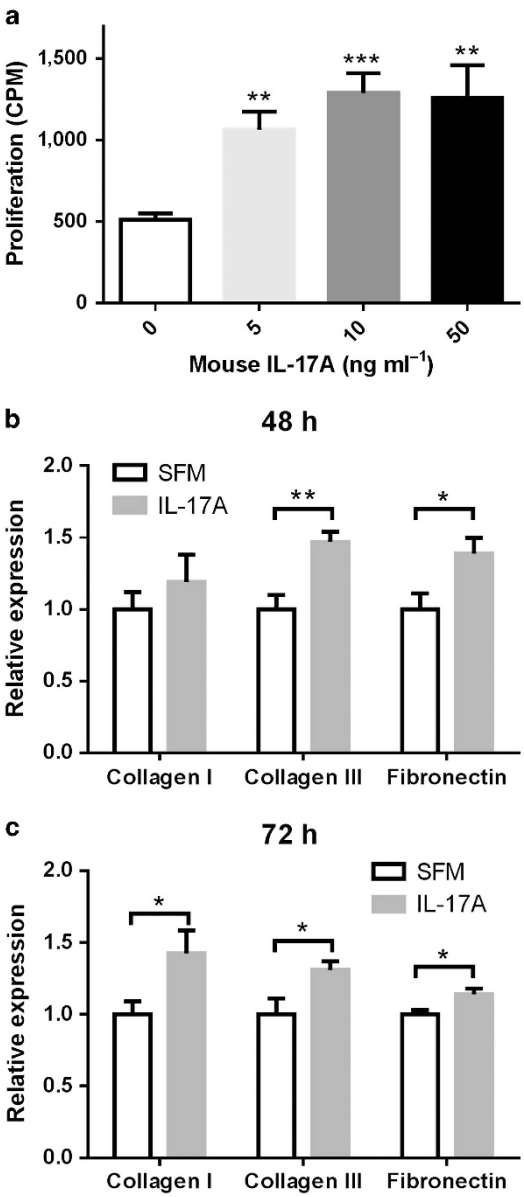

Figure 5 IL-17A directly activates lung mesenchymal cells. (**a**) Dose–response of mouse primary lung mesenchymal cell proliferation to recombinant murine IL-17A *in vitro* as measured by uptake of ^{3}H-thymidine (mean + s.e.m., $n = 10$). Each group was compared with the cells with solvent only. (**b**, **c**) Mouse primary mesenchymal cell mRNA expression of collagen types I and III and fibronectin in response to stimulation with 10 ng ml^{-1} recombinant murine IL-17A *in vitro* at 48 h (**b**) and 72 h (**c**). *$P < 0.05$, **$P < 0.01$ and ***$P < 0.001$. Similar results were seen in two additional experiments.

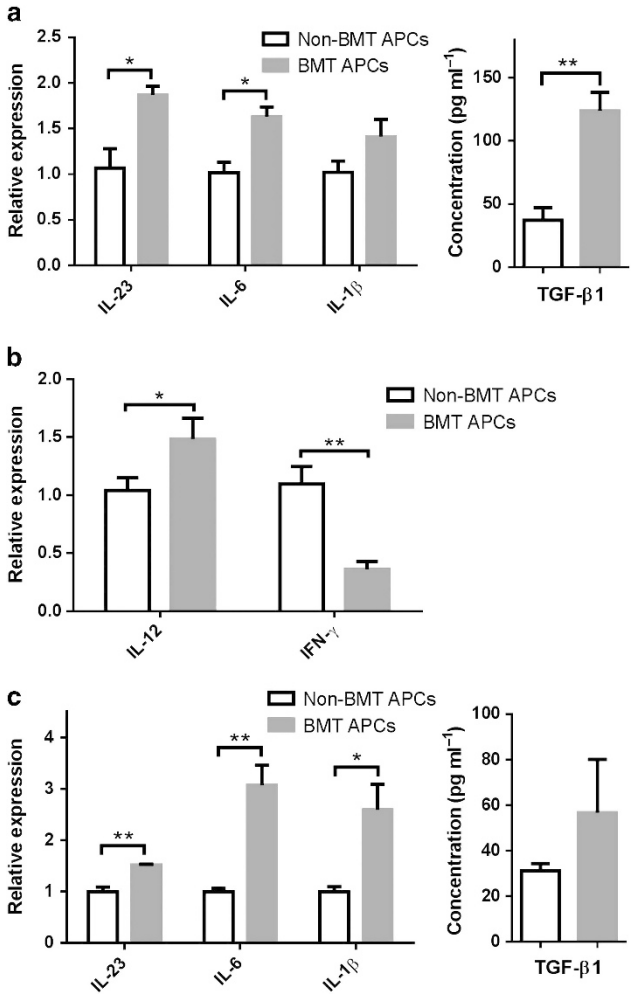

Figure 6 Altered cytokine expression in lung APCs from BMT mice in response to γHV-68 infection. (**a**) Expression of IL-6, IL-23 p19, IL-1β, and TGF-β1 in lung APCs from infected non-BMT or BMT mice. Lung CD11c^{+}-enriched APCs were isolated from non-BMT or BMT mice at 7 dpi. A total of 2×10^{6} lung APCs were seeded in a well of 24-well plate and restimulated with 0.25 multiplicity of infection (MOI) of γHV-68 for 36 h. Left, RT-PCR analysis of mRNA for IL-6, IL-23, and IL-1β in lung APCs (mean + s.e.m., $n = 4$); Right, ELISA for TGF-β1 in culture supernatant of lung APCs (mean + s.e.m., $n = 4$). (**b**) Expression of IL-12 p35 and IFN-γ mRNA in same cells as in (**a**). (**c**) Expression of IL-6, IL-23, IL-1β, and TGF-β1 in lung APCs from uninfected non-BMT or BMT mice. Lung CD11c+ APCs were enriched from uninfected non-BMT or BMT mice and were stimulated with 1 MOI virus *ex vivo* for 24 h. Left, RT-PCR analysis of mRNA of IL-6, IL-23, and IL-1β in lung APCs; Right, ELISA for TGF-β1 in culture supernatant of lung APCs (mean + s.e.m., $n = 3$). Similar results were obtained in two independent experiments.

21 dpi likely reflects clearance of the majority of the infected cells as this construct would still be predicted to be visible during latency owing to the slow degradation of this fusion protein.[15]

Another potential explanation for the exuberant development of lung pathology in the BMT mice involves persistent reactivation of virus as seen in T_H2-biased mice.[17] However, both cidofovir treatment starting at 5 dpi or use of the v-cyclin.stop virus, which initially replicates at levels equivalent to the WT virus before establishing latency[18] demonstrate that persistent viral reactivation is not relevant for this pathology. The reasons for the differences in these models (BMT vs. IFNγR$^{-/-}$ mice) may reflect that BMT mice are deficient, but not devoid of IFN-γ signaling, that there is no alteration in T_H2 cytokine responses in BMT mice or may reflect alterations caused by conditioning. Note that although irradiation alone can cause pulmonary fibrosis after ~9 months,[25] this is a much longer time frame than our experiments, and fibrosis and pneumonitis are not seen in our BMT mice in the absence of infection. Taken together, these results suggest the development

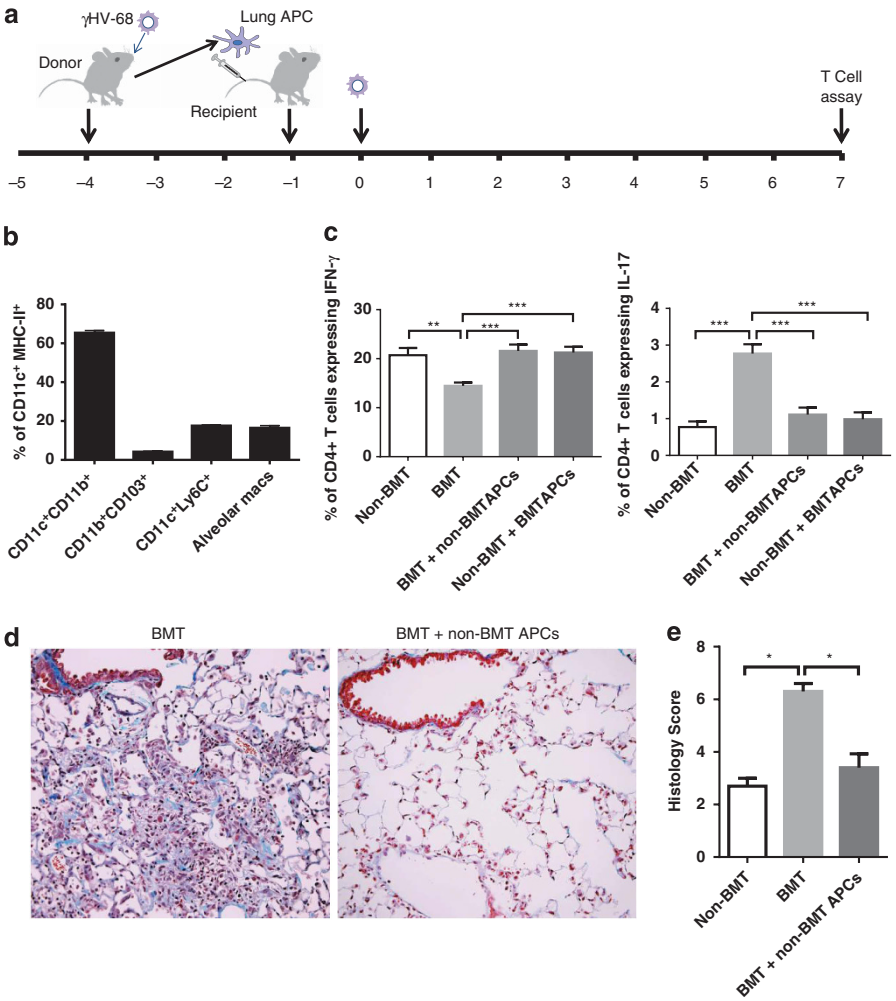

Figure 7 Lung APCs from non-BMT mice restore T_H1 and limit T_H17 response in BMT mice. (**a**) A scheme of adoptive transfer of lung APCs and γHV-68 infection. (**b**) Characterization of CD11c+ MHC class II+ cell population used for adoptive transfer. (**c**) The alteration of the percentage of CD4+ IFN-γ+ T_H1 cells and CD4+ IL-17A+ T_H17 cells by adoptive transfer of lung APCs. Lung CD11c+ APCs were enriched by magnetic beads from viral-infected non-transplanted or BMT mice, and adoptively transferred into BMT mice or non-transplanted mice, respectively. Single cell suspensions were prepared at 7 dpi for phorbol 12-myristate 13-acetate (PMA) stimulation and flow cytometry analysis. Left, percent of CD4+ cells that express IFN-γ (T_H1 cells, mean + s.e.m., $n=5$); Right, percent of CD4+ cells that express IL-17A (T_H17 cells, mean + s.e.m., $n=5$). (**d**) Representative Masson's trichrome staining on lung sections from BMT mice with or without adoptive transfer of primed non-BMT lung APCs at 21 dpi. The blue staining represents deposition of collagen. Same magnification was used for all images. (**e**) The average histology scores of lung sections from γHV-68 infected non-BMT, BMT mice, or BMT mice adoptively transferred with non-BMT lung APCs at 21 dpi (mean + s.e.m., $n=3$). $^*P<0.05$, $^{**}P<0.01$, $^{***}P<0.001$. Similar results were obtained in two (**b**, **d**, **e**) or three (**c**) independent experiments.

of fibrosis relates to an altered immune response rather than ongoing viral reactivation and that IL-17A can promote the development of lung pathology without impacting the degree of acute viral replication and early lung injury.

IL-17A has been implicated in mediating other forms of lung fibrosis and HSCT complications.[26–29] Under non-transplant conditions such as idiopathic pulmonary fibrosis, elevated levels of IL-17A are found in the bronchoalveolar lavage fluid.[26] Neutralization of IL-17A, IL-17A deficiency, or IL-17RA deficiency in mouse models attenuates lung fibrosis induced by bleomycin,[26,27] silica,[27] or *Saccharopolyspora rectivirgula*.[30] However, in our laboratory, *Il-17a*$^{-/-}$ mice develop equivalent bleomycin-induced fibrosis as WT mice (data not shown) and others have reported that IL-17A does not promote silica-induced lung fibrosis.[31] Thus, the ability of IL-17A to promote fibrosis may be context specific. Lung transplant patients who develop BOS have increased IL-17A in bronchoalveolar lavage fluid.[32] In allogeneic BMT mice, IFN-γ suppresses the production of IL-17A, which is responsible for severe acute IPS.[33] More recently, Varelias *et al.*[34] demonstrated local IL-6 secretion in the absence of IFN-γ drives expansion of donor alloantigen-specific T_H17 cells to promote acute IPS development in both murine models and human HSCT patients. However, the role of IL-17A in development of fibrosis during the chronic phase of IPS has not yet been investigated. Here we identified a critical role for IL-17A in viral-driven lung fibrosis and pneumonitis post HSCT. We found the increased levels of IL-17A in BMT mice directly contribute to fibrosis by stimulating proliferation and extracellular matrix synthesis in mesenchymal cells. We also considered the possibility that

the T_H17 response was promoting the development of pneumonitis and fibrosis via the recruitment of neutrophils to the lung. We observed a fourfold increase in neutrophils in the lung at 7 dpi, but there were no significant differences between BMT and non-BMT lungs analyzed at 10 dpi and afterwards (**Supplementary Figure 3a**). Furthermore, administration of neutrophil-specific depletion antibodies against Ly-6G[35] did not protect BMT mice from pneumonitis and pulmonary fibrosis at 21 dpi (**Supplementary Figure 3b**).

Consistent with the skewing of T_H17 differentiation, we found that lung APCs in BMT mice produce more pro-T_H17 response cytokines and fewer T_H1-promoting cytokines with the exception of IL-12 (**Figure 6a, b**). The BMT APCs show little evidence of cytokine alteration in the absence of infection (**Supplementary Figure 4a-b**), suggesting that γHV-68 is actively contributing to this phenotype. As BMT mice have higher early viral loads, we asked if different viral loads will contribute to the change of cytokine production by the APCs. When infecting BMT and non-BMT APCs *ex vivo* with the same high dose (multiplicity of infection = 1) of γHV-68, BMT APCs still secrete higher levels of T_H17-promoting cytokines than non-BMT DCs, suggesting an intrinsic alteration to the APCs in BMT mice. These data also suggest that IL-12 production by BMT APCs, accompanied with low levels of IFN-γ and high pro-T_H17 cytokines, is insufficient to promote viral-specific T_H1 responses. The CD4+ T cells themselves may also contribute to the skewing of T-cell differentiation. The process of BMT induces changes in repopulating T cells that may favor T_H17 as opposed to T_H1 differentiation. Support for an altered T-cell phenotype in BMT mice comes from the observation that BMT T cells do not proliferate well in a mixed lymphocyte response assay.[13] Thus, the influence of BMT on T-cell phenotype is a complex process and may involve not only lung APCs but also intrinsic T-cell differences.

Adoptive transfer of primed lung APCs from normal mice into BMT mice can correct the T_H1/T_H17 balance after γHV-68 infection, but adoptive transfer of APCs from BMT lungs into normal mice is not able to increase the level of T_H17 cells, likely because of the fact that the recipient mice still have endogenous non-BMT APCs available. Lung DCs include four main subsets: in an uninfected lung there are $CD11b^+$ conventional DCs, $CD103^+$ conventional DCs, and plasmacytoid DCs, whereas on inflammation, inflammatory monocyte-derived DCs are recruited to the lung.[36] It has been reported that T_H17-cell responses are induced by inflammatory DCs[37] and $CD103^+$ $CD11b^+$ tissue-resident DCs.[38,39] The major APCs in our adoptive transfer studies were CD11b+ conventional myeloid DCs, but a limitation to our study is that the transferred cell population was a mixture of APC types. How non-BMT APCs overpower BMT APCs in guiding CD4+ T helper-cell differentiation is not yet understood. When BMT lung APCs are adoptively transferred into non-BMT mice, the high levels of IFN-γ in non-BMT mice may work to suppress the pro-T_H17 effects of BMT lung APCs through suppression of their expression of IL-6.[33,34]

Prostaglandin E_2 has previously been shown to promote T_H1 to T_H17 skewing by DCs.[40,41] Prostaglandin E_2 can stimulate bone marrow-derived DCs to produce IL-23 and suppress IL-12 and thus promote T_H17 differentiation and maintenance.[40,42–44] Syngeneic BMT mice overexpress prostaglandin E_2 in the lungs both before and after viral infection.[13,45] However, the inhibition of prostaglandin synthesis using indomethacin post BMT did not alter clearance of lytic virus[13] and we now confirm that use of prostaglandin E_2 synthase-deficient mice[46] as BMT donors and/or recipients has no impact on T_H1/T_H17 balance or development of pneumonitis and fibrosis (**Supplementary Figure 5a,d**); however, it remains a formal possibility that other prostaglandins may be involved.

In summary, our data suggest preceding viral infections may be responsible for the later development of lung pathology in some HSCT recipients. Our mouse model of viral infection in BMT mice develops features of pneumonitis and fibrosis that are also noted in diseases like IPS, COP, and BOS. This is consistent with previous clinical studies, which suggest that a preceding respiratory viral infection may predict eventual development of lung pathology.[9,10] In contrast to these observations, however, are recent data from CMV prophylaxis studies that have not demonstrated benefit for prophylactic therapy versus therapy initiated once viral replication is detected[47] in prevention of end-stage CMV disease and death. Right now, it is hard to know whether prophylaxis against a single organism can be effective, or whether new therapies are needed that can be used earlier post transplant. Recently, sensitive testing of banked bronchoalveolar lavage fluid from IPS patients revealed a variety of previously unidentified pathogens in >56% of the total cases, with human herpes viruses-6 being found most frequently.[8] In addition, a trial of a new anti-CMV therapy, with reduced bone marrow toxicity allowing treatment to start sooner post HSCT, demonstrated that many patients were positive for viral replication before prophylactic therapy is routinely started.[48,49] Excitingly, this drug, letermovir, did show promise in limiting CMV end-stage disease. A final hopeful note is that our data, along with accumulating evidence from other studies mentioned above suggest that neutralization of IL-17A, may be an effective therapy to limit pneumonitis and fibrosis even when started late after disease onset.

METHODS

Mouse strains. C57BL/6J mice were purchased from the Jackson Laboratory (Bar Harbor, ME). B6.*Il-17a*$^{-/-}$ mice[20] and inducible prostaglandin synthase-deficient mice (*mPGEs*$^{-/-}$)[46] have been previously described and were bred in the animal facility of the University of Michigan, Ann Arbor, MI. Experiments were approved by the University of Michigan Committee on the Use and Care of Animals.

Syngeneic BMT. Recipient WT or B6.*Il-17a*$^{-/-}$ mice were treated with 13 Gy total body irradiation (split dose) using a ^{137}Cs irradiator, followed by tail vein injection of 5×10^6 whole-bone marrow cells from WT or B6. *Il-17a*$^{-/-}$ mice. Chimeras were infected with γHV-68 at the 5th week after BMT, when total numbers of hematopoietic cells were fully reconstituted in the lungs and spleen.[14]

γHV-68 infection and plaque assays. Non-BMT or BMT mice were infected with 5×10^4 pfu of murine γHV-68 (VR-1465, ATCC, Manassas, VA), γHV-68-H2bYFP[15] or v-cyclin-deficient γHV-68[18] intranasally after being anesthetized with ketamine and xylazine. To quantify lytic virus, right lungs were harvested and homogenized in 1 ml complete media. Supernatants were diluted and inoculated onto 3T12 cells (ATCC); plaques were enumerated 7 days later.

Lung cell preparation and flow cytometry. Single-cell suspensions of leukocytes were prepared from whole lungs by collagenase digestion for flow cytometry as described previously.[13] In brief, each minced lung was incubated in 15 ml of complete media with 1 mg ml^{-1} collagenase (Boehringer Mannheim Biochemical, Chicago, IL), and 17 U ml^{-1} DNase I (Sigma-Aldrich, St Louis, MO) for 30 min at 37 °C. The digested tissue was drawn through the bore of a 10-ml syringe repeatedly, and filtered through 100-μm mesh. Cells were stimulated with phorbol 12-myristate 13-acetate (PMA) (0.05 μg/ml; Sigma-Aldrich) and ionomycin (0.75 μg/ml; Sigma-Aldrich) for 4 h in the presence of GolgiStop protein transport inhibitor (BD Pharmingen, San Jose, CA) before intracellular cytokine staining. An aliquot of 1×10^6 cells was first blocked by anti-CD16/CD32 (Fc block; BD Pharmingen) antibodies and then stained using fluorochrome-conjugated antibodies against CD45, CD4, IL-17A, IL-4, or IFN-γ (BD Pharmingen). For characterization of lung APCs, flow cytometry was performed using antibodies specific for CD11c (N418), CD103 (2E7), I-A^b (AF6-120.1), and CD68 (FA-11), all from BioLegend (San Diego, CA); CD11b (M1/70, BD Pharmingen); and Ly6C (HK1.4) and F4/80 (BM8) from eBioscience (San Diego, CA). The fluorescein isothiocyanate channel was used to detect autofluorescence of alveolar macrophages.

Lung APC adoptive transfer. Single cell suspensions were prepared from whole lungs and mediastinal lymph nodes by collagenase digestion. Macrophages were reduced from the suspensions by 90-min adherence on tissue culture plastic. CD11c+ cells were then positively selected by using anti-mouse CD11c magnetic microbeads and columns (Miltenyi Biotec, Auburn, CA). A total of 5×10^5 CD11c+ lung APCs were injected into recipients via tail vein.

***In vivo* neutralization of IL-17A**. Rabbit polyclonal antibodies against mouse IL-17A were generated and specificity of the antibodies was tested using a direct enzyme-linked immunosorbent assay to IL-17A as well as other IL-17 family members.[50] A dose of 2.5 mg of purified polyclonal anti-mouse IL-17A or rabbit immunoglobulin G isotype was injected intraperitoneally at designated time points.

Cidovfovir treatment. Cidofovir (Mylan, Institutional LLC) was administered subcutaneously at a dose of 25 mg/kg of body weight. Mice were treated for 2 consecutive days starting at the designated date and then were injected in every 3 days until 21 dpi.

Lung section staining and microscopy. For immunofluorescence staining, frozen lung sections were fixed in 3.7% formaldehyde, followed by blocking with 1% bovine serum albumin in phosphate-buffered saline, and stained with a chicken anti-GFP primary antibody (Abcam, Cambridge, MA) and an Alexa Fluor 488 conjugated goat anti-chicken secondary antibody (Life technology, Carlsbad, CA). Images were collected on a Zeiss ApoTome fluorescent microscope using AxioVision software. For hematoxylin and eosin staining or Masson's trichrome staining, whole lungs were inflated and fixed with 10% buffered formalin, dehydrated by ethanol and embedded in paraffin. Sections were cut at a thickness of 3 μm, mounted on glass slides, and stained using hematoxylin and eosin or Masson's trichrome. Images were taken on a Olympus BX-51 microscope by a DP-70 camera.

Quantitative reverse transcriptase PCR. The relative amount of mRNA for target genes was assayed by real-time reverse transcriptase PCR using thermocycler ABI Prism 7000 (Applied Biosystems, Foster City, CA) using a previously described protocol.[45] Gene-specific primers and probes (**Table 1**) were designed using Primer Express software (Applied Biosystems).

Table 1 Primers and probes for semiquantitative real-time RT-PCR

Gene	Oligo	Primer sequence
DNA polymerase (ORF9)	Forward	5′-ACAGCAGCTGGCCATAAAGG-3′
	Reverse	5′-TCCTGCCCTGGAAAGTGATG-3′
	Probe	5′-CCTCTGGAATGTTGCCTTGCCTCCA-3′
β-actin	Forward	5′-CCGTGAAAAGATGACCCAGATC-3′
	Reverse	5′-CACAGCCTGGATGGCTACGT-3′
	Probe	5′-TTTGAGACCTTCAACACCCCCAGCCA-3′
Collagen I	Forward	5′-TGACTGGAAGAGCGGAGAGTACT-3′
	Reverse	5′-GGTCTGACCTGTCTCCATGTTG-3′
	Probe	5′-CTGCAACCTGGACGCCATCAAGG-3′
Collagen III	Forward	5′-GGATCTGTCCTTTGCGATGAC-3′
	Reverse	5-GCTGTGGGCATATTGCACAA-3′
	Probe	5′-TGCCCCAACCCAGAGATCCCATTT-3′
Fibronectin	Forward	5′-TCGAGCCCTGAGGATGGA-3′
	Reverse	5′-GTGCAAGGCAACCACACTGA-3′
	Probe	5′-CTGCAGGGCCTCAGGCCGG-3′
IL-23 p19	Forward	5′-CTCCCTACTAGGACTCAGCCAACT-3′
	Reverse	5′-ACTCAGGCTGGGCATCTGTT-3′
	Probe	5′-AGCCAGAGGATCACCCCCGGG-3′
IL-6	Forward	5′-GACTTCCATCCAGTTGCCTTCT-3′
	Reverse	5′-CTGTTGGGAGTGGTATCCTCTGT-3′
	Probe	5′-TGACAACCACGGCCTTCCCTACTTCA-3′
IL-1β	Forward	5′-GAGCCCATCCTCTGTGACTCA-3′
	Reverse	5′-GTTGTTCATCTCGGAGCCTGTAG-3′
	Probe	5′-AACCTGCTGGTGTGTGACGTTCCCA-3′
IL-12 p35	Forward	5′-GTTGCCTGGCTACTAGAGAGACTTC-3′
	Reverse	5′-GCACAGGGTCATCATCAAAGAC-3′
	Probe	5′-ACAACAAGAGGGAGCTGCCTGCC-3′
IFN-γ	Forward	5′-GCAACAGCAAGGCGAGAAA-3′
	Reverse	5′-GCTGGATTCCGGCAACAG-3′
	Probe	5′-AGGTCAACAACCCACAGGTCCAGCG-3′

Abbreviations: IFN-γ, interferon-γ; IL, interleukin.

Enzyme-linked immunosorbent assay. Enzyme-linked immunosorbent assay for active transforming growth factor beta was performed using R&D Systems kits according to manufacturer's instructions.

Histologic scores. Histologic sections stained with hematoxylin and eosin and trichrome were scored in a blinded fashion by a lung pathologist (Dr Konopka) as described previously.[12] Lungs were scored for severity of fibrosis, perivascular inflammation, peripheral inflammation, presence, or absence of foamy alveolar macrophages and intra-alveolar fibrin. The scores for each factor were added to give a pathology score, with 11 indicating the most severe phenotype.

Mesenchymal cell assays. Mesenchymal cells were isolated from lung minces of non-BMT mice following 2 weeks of culture. Proliferation assays utilized 5000 mesenchymal cells/well in 96-well plates in serum-free media treated with the indicated concentrations of IL-17A for 48 h prior to addition of ^{3}H-thymidine and determination of radiolabeled DNA in the nucleus as a measure of cellular

proliferation. For measurement of extracellular matrix, 4×10^5 mesenchymal cells were cultured in serum-free media in the presence of IL-17A for 48 or 72 h prior to the collection of total cellular RNA and analysis of collagen 1, collagen 3, and fibronectin by real-time reverse transcriptase PCR.

Statistical analysis. When groups of two were compared, student's *t*-tests were used to determine significance; when groups of three or more were compared, analysis of variance was utilized with a Tukey's multiple comparisons test to determine significance.

Supplementary Material is linked to the online version of the paper at http://www.nature.com/mi

ACKNOWLEDGMENTS

This work was supported by NIH grant AI117229 and HL115618 awarded to B.B.M. X.Z. and S.G. were supported by T32HL07749. X.Z. was also supported by Post-doctoral translational scholar grant from MICHR 2UL1TR000433. S.C. was supported by T32 AI007413 at the time of this work when she was at the University of Michigan. We are also grateful to Dr Sam Speck from Emory University who provided the γHV-68-H2bYFP virus for these studies.

DISCLOSURE

The authors declare no conflict of interest.

REFERENCES

1. Afessa, B. & Peters, S.G. Major complications following hematopoietic stem cell transplantation. *Semin. Respir. Crit. Care. Med.* **27**, 297–309 (2006).
2. Soubani, A.O. & Pandya, C.M. The spectrum of noninfectious pulmonary complications following hematopoietic stem cell transplantation. *Hematol. Oncol. Stem. Cell. Ther.* **3**, 143–157 (2010).
3. Passweg, J.R. *et al.* Hematopoietic SCT in Europe: data and trends in 2012 with special consideration of pediatric transplantation. *Bone Marrow Transplant.* **49**, 744–750 (2014).
4. Wingard, J.R., Hsu, J. & Hiemenz, J.W. Hematopoietic stem cell transplantation: an overview of infection risks and epidemiology. *Infect. Dis. Clin. North. Am.* **24**, 257–272 (2010).
5. Yoshihara, S., Yanik, G., Cooke, K.R. & Mineishi, S. Bronchiolitis obliterans syndrome (BOS), bronchiolitis obliterans organizing pneumonia (BOOP), and other late-onset noninfectious pulmonary complications following allogeneic hematopoietic stem cell transplantation. *Biol. Blood Marrow Transplant.* **13**, 749–759 (2007).
6. Uhlving, H.H. *et al.* Biopsy-verified bronchiolitis obliterans and other noninfectious lung pathologies after allogeneic hematopoietic stem cell transplantation. *Biol. Blood Marrow Transplant.* **21**, 531–538 (2014).
7. Panoskaltsis-Mortari, A. *et al.* An official American Thoracic Society research statement: noninfectious lung injury after hematopoietic stem cell transplantation: idiopathic pneumonia syndrome. *Am. J. Respir. Crit. Care. Med.* **183**, 1262–1279 (2011).
8. Seo, S. *et al.* Idiopathic pneumonia syndrome after hematopoietic cell transplantation: evidence of occult infectious etiologies. *Blood* **125**, 3789–3797 (2015).
9. Erard, V. *et al.* Airflow decline after myeloablative allogeneic hematopoietic cell transplantation: the role of community respiratory viruses. *J. Infect. Dis.* **193**, 1619–1625 (2006).
10. Versluys, A.B., Rossen, J.W., van Ewijk, B., Schuurman, R., Bierings, M.B. & Boelens, J.J. Strong association between respiratory viral infection early after hematopoietic stem cell transplantation and the development of life-threatening acute and chronic alloimmune lung syndromes. *Biol. Blood Marrow Transplant.* **16**, 782–791 (2010).
11. Moore, B.B. & Moore, T.A. Viruses in idiopathic pulmonary fibrosis: etiology and exacerbation. *Ann. Am. Thorac. Soc.*, in press (2015).
12. Coomes, S.M., Farmen, S., Wilke, C.A., Laouar, Y. & Moore, B.B. Severe gammaherpesvirus-induced pneumonitis and fibrosis in syngeneic bone marrow transplant mice is related to effects of transforming growth factor-beta. *Am. J. Pathol.* **179**, 2382–2396 (2011).
13. Coomes, S.M., Wilke, C.A., Moore, T.A. & Moore, B.B. Induction of TGF-beta 1, not regulatory T cells, impairs antiviral immunity in the lung following bone marrow transplant. *J. Immunol.* **184**, 5130–5140 (2010).
14. Hubbard, L.L., Ballinger, M.N., Wilke, C.A. & Moore, B.B. Comparison of conditioning regimens for alveolar macrophage reconstitution and innate immune function post bone marrow transplant. *Exp. Lung Res.* **34**, 263–275 (2008).
15. Collins, C.M. & Speck, S.H. Tracking murine gammaherpesvirus 68 infection of germinal center B cells *in vivo*. *PloS One* **7**, e33230 (2012).
16. Vannella, K.M., Luckhardt, T.R., Wilke, C.A., van Dyk, L.F., Toews, G.B. & Moore, B.B. Latent herpesvirus infection augments experimental pulmonary fibrosis. *Am. J. Respir. Crit. Care. Med.* **181**, 465–477 (2010).
17. Mora, A.L. *et al.* Control of virus reactivation arrests pulmonary herpesvirus-induced fibrosis in IFN-gamma receptor-deficient mice. *Am. J. Respir. Crit. Care. Med.* **175**, 1139–1150 (2007).
18. van Dyk, L.F., HWt, Virgin & Speck, S.H. The murine gammaherpesvirus 68 v-cyclin is a critical regulator of reactivation from latency. *J. Virol.* **74**, 7451–7461 (2000).
19. Lea, A.P. & Bryson, H.M. Cidofovir. *Drugs* **52**, 225–230. discussion 231 (1996).
20. Nakae, S. *et al.* Antigen-specific T cell sensitization is impaired in IL-17-deficient mice, causing suppression of allergic cellular and humoral responses. *Immunity* **17**, 375–387 (2002).
21. Lukacs, N.W., Smit, J.J., Mukherjee, S., Morris, S.B., Nunez, G. & Lindell, D.M. Respiratory virus-induced TLR7 activation controls IL-17-associated increased mucus via IL-23 regulation. *J. Immunol.* **185**, 2231–2239 (2010).
22. Yao, Z. *et al.* Herpesvirus Saimiri encodes a new cytokine, IL-17, which binds to a novel cytokine receptor. *Immunity* **3**, 811–821 (1995).
23. Holt, P.G. & Batty, J.E. Alveolar macrophages. V. Comparative studies on the antigen presentation activity of guinea-pig and rat alveolar macrophages. *Immunology* **41**, 361–366 (1980).
24. Doherty, P.C., Christensen, J.P., Belz, G.T., Stevenson, P.G. & Sangster, M.Y. Dissecting the host response to a gamma-herpesvirus. *Philos. Trans. R. Soc. Lond. B. Biol. Sci.* **356**, 581–593 (2001).
25. Travis, E.L., Down, J.D., Holmes, S.J. & Hobson, B. Radiation pneumonitis and fibrosis in mouse lung assayed by respiratory frequency and histology. *Radiat. Res.* **84**, 133–143 (1980).
26. Wilson, M.S. *et al.* Bleomycin and IL-1beta-mediated pulmonary fibrosis is IL-17A dependent. *J. Exp. Med.* **207**, 535–552 (2010).
27. Mi, S. *et al.* Blocking IL-17A promotes the resolution of pulmonary inflammation and fibrosis via TGF-beta1-dependent and -independent mechanisms. *J. Immuno.l* **187**, 3003–3014 (2011).
28. Lei, L., Zhong, X.N., He, Z.Y., Zhao, C. & Sun, X.J. IL-21 Induction of CD4+ T cell differentiation into Th17 cells contributes to bleomycin-induced fibrosis in mice. *Cell Biol Int.* **39**, 388–399 (2014).
29. Francois, A. *et al.* B cell activating factor is central to bleomycin- and IL-17-mediated experimental pulmonary fibrosis. *J. Autoimmun.* **56**, 1–11 (2014).
30. Simonian, P.L. *et al.* Th17-polarized immune response in a murine model of hypersensitivity pneumonitis and lung fibrosis. *J. Immunol.* **182**, 657–665 (2009).
31. Lo, R.e.S. *et al.* IL-17A-producing gammadelta T and Th17 lymphocytes mediate lung inflammation but not fibrosis in experimental silicosis. *J. Immunol.* **184**, 6367–6377 (2010).
32. Vanaudenaerde, B.M. *et al.* The role of the IL23/IL17 axis in bronchiolitis obliterans syndrome after lung transplantation. *Am. J. Transplant.* **8**, 1911–1920 (2008).
33. Mauermann, N. *et al.* Interferon-gamma regulates idiopathic pneumonia syndrome, a Th17+CD4+ T-cell-mediated graft-versus-host disease. *Am. J. Respir. Crit. Care Med.* **178**, 379–388 (2008).
34. Varelias, A. *et al.* Lung parenchyma-derived IL-6 promotes IL-17A-dependent acute lung injury after allogeneic stem cell transplantation. *Blood* **125**, 2435–2444 (2015).
35. Daley, J.M., Thomay, A.A., Connolly, M.D., Reichner, J.S. & Albina, J.E. Use of Ly6G-specific monoclonal antibody to deplete neutrophils in mice. *J. Leukoc. Biol.* **83**, 64–70 (2008).

36. Neyt, K. & Lambrecht, B.N. The role of lung dendritic cell subsets in immunity to respiratory viruses. *Immunol Rev* **255**, 57–67 (2013).
37. Segura, E. *et al.* Human inflammatory dendritic cells induce Th17 cell differentiation. *Immunity* **38**, 336–348 (2013).
38. Schlitzer, A. *et al.* IRF4 transcription factor-dependent CD11b+ dendritic cells in human and mouse control mucosal IL-17 cytokine responses. *Immunity* **38**, 970–983 (2013).
39. Persson, E.K. *et al.* IRF4 transcription-factor-dependent CD103(+) CD11b(+) dendritic cells drive mucosal T helper 17 cell differentiation. *Immunity* **38**, 958–969 (2013).
40. Sheibanie, A.F. *et al.* The proinflammatory effect of prostaglandin E2 in experimental inflammatory bowel disease is mediated through the IL-23–>IL-17 axis. *J. Immunol.* **178**, 8138–8147 (2007).
41. Boniface, K. *et al.* Prostaglandin E2 regulates Th17 cell differentiation and function through cyclic AMP and EP2/EP4 receptor signaling. *J. Exp. Med.* **206**, 535–548 (2009).
42. Sheibanie, A.F., Tadmori, I., Jing, H., Vassiliou, E. & Ganea, D. Prostaglandin E2 induces IL-23 production in bone marrow-derived dendritic cells. *FASEB J.* **18**, 1318–1320 (2004).
43. Khayrullina, T., Yen, J.H., Jing, H. & Ganea, D. *In vitro* differentiation of dendritic cells in the presence of prostaglandin E2 alters the IL-12/IL-23 balance and promotes differentiation of Th17 cells. *J. Immunol.* **181**, 721–735 (2008).
44. Poloso, N.J., Urquhart, P., Nicolaou, A., Wang, J. & Woodward, D.F. PGE2 differentially regulates monocyte-derived dendritic cell cytokine responses depending on receptor usage (EP2/EP4). *Mol. Immunol.* **54**, 284–295 (2013).
45. Ballinger, M.N. *et al.* Critical role of prostaglandin E2 overproduction in impaired pulmonary host response following bone marrow transplantation. *J. Immunol.* **177**, 5499–5508 (2006).
46. Trebino, C.E. *et al.* Impaired inflammatory and pain responses in mice lacking an inducible prostaglandin E synthase. *Proc. Natl Acad Sci. USA* **100**, 9044–9049 (2003).
47. Boeckh, M. *et al.* Valganciclovir for the prevention of complications of late cytomegalovirus infection after allogeneic hematopoietic cell transplantation: a randomized trial. *Ann. Intern. Med.* **162**, 1–10 (2015).
48. Griffiths, P.D. & Emery, V.C. Taming the transplantation troll by targeting terminase. *N. Engl. J. Med.* **370**, 1844–1846 (2014).
49. Chemaly, R.F. *et al.* Letermovir for cytomegalovirus prophylaxis in hematopoietic-cell transplantation. *N. Engl. J. Med.* **370**, 1781–1789 (2014).
50. Mukherjee, S. *et al.* IL-17-induced pulmonary pathogenesis during respiratory viral infection and exacerbation of allergic disease. *Am. J. Pathol.* **179**, 248–258 (2011).